Check for updates

Geophysical Research Letters

RESEARCH LETTER
10.1029/2025GL116411

Special Collection:
Slow to fast earthquakes and the geology, structure, and rheology of their host subduction zones

Analysis of Shear Wave Splitting Patterns in Alaska: Evidence for Strong Intra-Slab Anisotropy

Sharmila Appini[1], Yingcai Zheng[1], Jonny Wu[2], and Walter D. Mooney[3]

[1]Department of Earth and Atmospheric Sciences, University of Houston, Houston, TX, USA, [2]Department of Geosciences, University of Arizona, Tucson, AZ, USA, [3]U.S. Geological Survey, Moffett Field, CA, USA

Abstract Shear wave splitting (SWS) patterns at subduction zones are often interpreted by complex mantle flow above or below the slab. However, our recent previous work shows dipping anisotropic slabs can explain observed patterns in Japan. Here, we extend this analysis to the Alaska subduction zone, using 2,567 high-quality teleseismic SWS measurements from 195 broadband stations. As was found in Japan, the observed SWS patterns in Alaska depend on earthquake backazimuth. The fast-S polarization directions are either trench parallel or perpendicular in southeastern Alaska and form a prominent circular pattern in central Alaska. We found that a dipping anisotropic slab following the Slab 2.0 geometry, with 30% shear anisotropy, and exhibiting tilted transverse isotropy with a symmetry axis normal to the slab interface, predicts both the fast-S polarizations and delay times (δt = 1.0–1.5 s). This suggests that intra-slab anisotropy can be the primary control on SWS, without requiring complex mantle flow.

Plain Language Summary Understanding seismic anisotropy within subducting slabs is essential for deciphering deep earthquake rupture processes and associated stress conditions. Shear wave splitting (SWS) has traditionally been linked to large-scale mantle flow, but the contribution of the slab itself remains under-explored. Our recent study indicates that subducting slabs can exhibit up to ~30% shear anisotropy, raising the question of whether this intrinsic slab property can account for complex SWS observations. In this study, we analyze 2,567 SWS measurements from teleseismic earthquakes recorded in the Alaska subduction zone. Our findings show that fast-S wave polarization directions vary systematically with earthquake location, implying that raypath incidence angle at the slab and intra-slab anisotropy might be key controlling factors. Forward modeling confirms that a dipping slab with significant anisotropy, likely due to mineral alignment and hydration, effectively reproduces the observed patterns. These results challenge conventional interpretations of SWS, highlighting the importance of considering slab anisotropy in subduction zone dynamics and mantle flow studies.

Key Points:

- We obtained 2,567 Shear wave splitting measurements using teleseismic SKS, SKKS, ScS, and S waves recorded by broadband stations across Alaska
- The observed splitting patterns can be explained by the dipping slab with ~30% shear anisotropy, consistent with local moment tensor analyses

Supporting Information:

Supporting Information may be found in the online version of this article.

Correspondence to:

S. Appini,
sappini@uh.edu

Citation:

Appini, S., Zheng, Y., Wu, J., & Mooney, W. D. (2025). Analysis of shear wave splitting patterns in Alaska: Evidence for strong intra-slab anisotropy. *Geophysical Research Letters*, *52*, e2025GL116411. https://doi.org/10.1029/2025GL116411

Received 9 APR 2025
Accepted 27 SEP 2025

Author Contributions:

Conceptualization: Sharmila Appini, Yingcai Zheng, Walter D. Mooney
Data curation: Sharmila Appini
Formal analysis: Sharmila Appini, Yingcai Zheng, Jonny Wu, Walter D. Mooney
Funding acquisition: Yingcai Zheng, Walter D. Mooney
Investigation: Sharmila Appini, Yingcai Zheng, Jonny Wu, Walter D. Mooney
Methodology: Sharmila Appini, Yingcai Zheng
Project administration: Yingcai Zheng
Resources: Yingcai Zheng

© 2025. The Author(s).
This is an open access article under the terms of the Creative Commons Attribution License, which permits use, distribution and reproduction in any medium, provided the original work is properly cited.

1. Introduction

Intermediate and deep earthquakes, defined as those earthquakes with depths greater than 70 km, occur within subducting slabs whereas most of the Earth's mantle is aseismic (Frohlich, 2006). Their occurrences pose a longstanding puzzle in seismology, as the brittle failure mechanism is not expected at those depths (Kirby et al., 1991). Investigating physical and chemical properties of the subducting slab, including anisotropy, can help identify whether deep earthquakes are linked to inherited fabric, phase transitions, or dehydration reactions that weaken the slab (e.g., Li et al., 2018; Shirey et al., 2021). Shear wave splitting (SWS)—where a seismic shear wave splits into two orthogonally polarized waves after passing an anisotropic medium—offers a direct probe of intra-slab anisotropy. SWS measurements have long been used to infer mantle flow patterns, since aligned crystals (e.g., olivine) or inclusions with an elastic contrast in the mantle, could generate seismic anisotropy (Long and Silver, 2009; Silver and Chan, 1991).

In many subduction zones, the observed fast-S polarization directions are often classified as trench-perpendicular or trench-parallel, which has led researchers to propose geodynamic flow models to interpret them—for example, the 2-D corner flow model, as well as toroidal mantle flow around slab edges driven by trench migration (Long and Silver, 2009; Perttu et al., 2014). Such a binary classification is probably an oversimplification, as evidenced by other studies and our prior SWS work in the Ryukyu subduction zone (e.g., Appini, Li, et al., 2025; Faccenda et al., 2008; Nowacki et al., 2015). Based on >7,000 SWS measurements in Japan, we found that fast-S polarization directions systematically change from trench-parallel to trench-perpendicular as a function of the earthquake backazimuth.

Software: Sharmila Appini, Yingcai Zheng
Supervision: Yingcai Zheng
Validation: Sharmila Appini, Yingcai Zheng, Jonny Wu, Walter D. Mooney
Visualization: Sharmila Appini
Writing – original draft: Sharmila Appini
Writing – review & editing: Sharmila Appini, Yingcai Zheng, Jonny Wu, Walter D. Mooney

Rather than invoking complex mantle flow above and below the slab to interpret the splitting observations, we found that strong seismic anisotropy within the subducting slab itself (i.e., intra-slab anisotropy) can reproduce the observed SWS patterns in Ryukyu, both in terms of the fast-S wave polarizations and delay times (Appini, Li, et al., 2025). Here, the term "slab" means the subducting oceanic lithosphere (crust and lithospheric mantle). This interpretation is in sharp contrast to the conventional view that intra-slab anisotropy contributes minimally to SWS because the seismic ray path length through the slab is relatively short compared to the much longer path in the upper mantle (Eakin et al., 2016). Thus, previous researchers have attributed observed SWS patterns to originate from above (Levin et al., 2002) or below the slab (Lynner et al., 2017; Song and Kawakatsu, 2012, 2013). In the Ryukyu subduction zone, our full-wave modeling predicts that a dipping slab with ∼30% anisotropy with a symmetry axis perpendicular to the slab surface, can explain the observed SWS observations (Appini, Li, et al., 2025). These modeling results demonstrate the importance of considering the presence of strong intra-slab anisotropy, resulting in alternative interpretations of mantle dynamics.

Li et al. (2018) carried out a global analysis of deep and intermediate-depth earthquake moment tensors (MTs) (Dziewonski et al., 1981; Ekström et al., 2012) in six subduction systems (including Alaska). They found that the observed seismic non-double-couple (non-DC) radiation patterns (or MTs) were best explained by shear dislocations on planar faults embedded in a highly anisotropic, laminated rock fabric surrounding the earthquakes within the slab. The global existence of non-DC components was further confirmed by Sawade et al. (2022) even after incorporating realistic 3D mantle heterogeneities. Two deep-earthquake regions in the Alaska-Aleutian slab were estimated by Li et al. (2018) to have a shear wave anisotropy strength γ of up to $\sim 35 \pm 6\%$ and $\sim 36 \pm 5\%$, respectively. Using 3D elastic finite difference modeling, Li et al. (2018) further showed that sub-slab anisotropy alone (i.e., assuming deep earthquake region is isotropic) cannot cause the observed non-DC components of the MTs.

Following our previous study of the Ryukyu subduction zone (Appini, Li, et al., 2025), we extend our investigation to Alaska, another major subduction zone, to test whether the dipping intra-slab anisotropy found by Li et al. (2018) can explain the observed SWS patterns. It would be appealing to see that intra-slab anisotropy can simultaneously account for both non-DC components of the deep earthquake MTs in slabs and the recorded SWS patterns of the shear waves passing through the slab at subduction zones. The Alaska-Aleutian subduction zone provides an excellent tectonic setting to investigate this hypothesis, as the Pacific plate subducts beneath North America along an arc of 50° in longitude (or ∼4,000 km) from the Aleutian Islands in the west to mainland Alaska in the east (Figure 1a). Along this arcuate subduction zone, the slab geometry varies from a steep dip beneath the central Aleutians to a shallower dip under south-central Alaska. In addition, abrupt slab edges are formed at both the eastern and western ends.

Previous SWS studies in Alaska have noted both trench-parallel and trench-perpendicular fast directions with delay times of 0.3–1.5 s, interpreted as evidence for multiple anisotropic sources and complex mantle flow patterns (e.g., Christensen and Abers, 2010; McPherson et al., 2020; Venereau et al., 2019; Yang et al., 2021). An interesting aspect in the south-central region is the subduction of the Yakutat terrane (Figure 1a), a buoyant oceanic plateau, which strongly influences both plate deformation (Haynie and Jadamec, 2024) and fast-S wave polarization directions, aligning with its subduction orientation. It is suggested that trench-parallel flow dominates beneath the Aleutian arc, likely driven by the normal-dipping Pacific slab rollback, while trench-normal fast S orientations in south-central Alaska indicate entrained flow beneath the shallow-dipping Yakutat slab (Jin et al., 2024). Near the Pacific-Yakutat slab edge, a circular pattern of fast S wave orientations is observed and attributed to an edge-induced toroidal flow system (Lynner et al., 2024; McPherson et al., 2020; Venereau et al., 2019; Yang et al., 2021). Z. Liu et al. (2025) further identified layered anisotropy in Alaska, which they attribute to sub-slab mantle flow, corner flow in the mantle wedge, and pre-existing fabrics within the subducting slab. These findings tried to understand the interplay between slab subduction, Yakutat terrane accretion and mantle flow (e.g., Jin et al., 2024).

Song and Kawakatsu (2013) challenged the prevailing view that mantle wedge anisotropy controls SKS splitting in Alaska (e.g., Liang et al., 2023; Perttu et al., 2014). They argued that tilted anisotropy in the sub-slab asthenosphere was mainly responsible for the observed SWS patterns, including a 90° shift in fast directions and backazimuthal dependence. They ruled out the role of slab on the grounds that its anisotropy derived from surface wave analyses is too small to explain the splitting times. However, in light of strong intra-slab anisotropy, we need to reconsider this analysis and interpretation.

19448007, 2025, 20, Downloaded from https://agupubs.onlinelibrary.wiley.com/doi/10.1029/2025GL116411 by Yingcai Zheng - University of Houston , Wiley Online Library on [12/11/2025]. See the Terms and Conditions (https://onlinelibrary.wiley.com/terms-and-conditions) on Wiley Online Library for rules of use; OA articles are governed by the applicable Creative Commons License

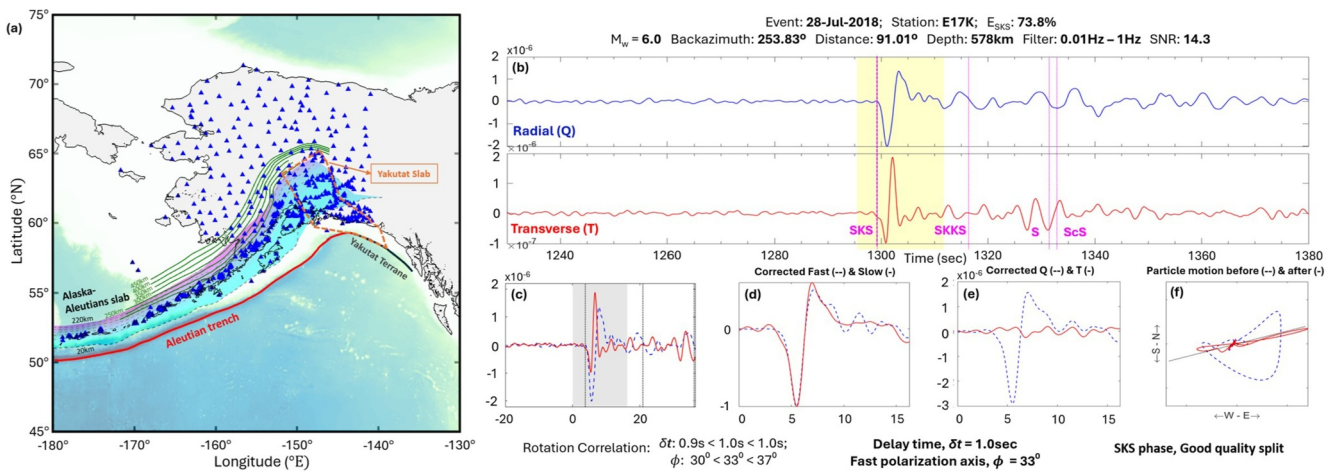

Figure 1. (a) Distribution of 673 seismic stations across Alaska (blue triangles). Alaska-Aleutian top slab geometry from the Slab 2.0 model (Hayes et al., 2018) is shown by cyan-magenta region and slab depth contours (black dashed lines) correspond to 20, 60, 100, 140, 180, and 220 km depths. The dark green lines with depth values denote the slab contours estimated from the isotropic V_p tomographic results of Gou et al. (2019). The orange dashed line denotes the extent of the Yakutat slab from Eberhart-Phillips et al. (2006) (b) QT components—radial (Q or SV) and transverse (T or SH) components. The highlighted (yellow) region indicates the data window used for shear wave splitting measurement; (c) raw Q (blue dashed) and T (red solid) waveforms prior to anisotropy correction; (d) fast (blue dashed) and slow (red solid) components after anisotropy correction; (e) Q (blue dashed) and T (red solid) components after the correction; (f) particle motion: elliptical (blue dashed) before correction and linearized (red solid) after correction.

In this study, we present a new data set of teleseismic SWS measurements for the Alaska subduction zone and evaluate the prediction capability of the intra-slab anisotropy model by Li et al. (2018) using the Slab2.0 model (Hayes et al., 2018). We then discuss the implications of our findings for subduction zone processes.

2. Data and Methods

We obtained broadband waveforms for teleseismic earthquakes from IRIS-DMC (March 2004–January 2020, $M_w > 5.5$, epicentral distances 30°–130°) and preprocessed them using ObsPy (Beyreuther et al., 2010). The waveform data is collected from the USArray and other local networks, with each record spanning 20 min, beginning 10–30 min after the earthquake origin time. Prior to the SWS analysis, the instrument response was removed from the seismograms and a zero-phase Butterworth band-pass filter with corner frequencies of 0.01 and 1.00 Hz was applied. We then applied the SplitLab software package (Wüstefeld et al., 2008a, 2008b) to determine the fast S-wave polarization direction and the delay time. These SWS measurements were performed using the rotation-correlation (Bowman and Ando, 1987; Fukao, 1984) method. To ensure high-quality SWS measurements, we apply multiple criteria for the analysis: a maximum correlation coefficient above 0.8, linearized particle motion after rotation, and measurement consistency with the eigenvalue method (Savage, 1999; Silver and Chan, 1991). Despite these measures, reported errors in our data set (Data set S1) may be underestimated, as noted by Walsh et al. (2013). We classify each SWS measurement and assign a quality rating as "good," "fair," or "poor" based on waveform quality, particle motion characteristics, and agreement among different splitting measurement techniques verified through visual inspection. Null measurements were also included in the data set, where no splitting was observed. We have examined more than 40,000 earthquake-station waveforms and obtained 2,567 high-confidence ("good" and "fair") SWS measurements of teleseismic SKS, SKKS, ScS, and S, including null values, at 195 seismic stations located in Alaska. Figures 1b–1f display seismic waveforms recorded at station E17K from a deep earthquake at 578 km depth, serving as an example to illustrate our shear-wave splitting (SWS) measurement procedure. A detailed description of the analysis can be found in Text S1 in Supporting Information S1. Our SWS data set, provided as Supporting Information S1, includes event and station details, event backazimuth, incidence angle at the station, splitting time, fast-S polarization, and measurement quality ratings.

19448007, 2025, 20, Downloaded from https://agupubs.onlinelibrary.wiley.com/doi/10.1029/2025GL116411 by Yingcai Zheng - University of Houston , Wiley Online Library on [12/11/2025]. See the Terms and Conditions (https://onlinelibrary.wiley.com/terms-and-conditions) on Wiley Online Library for rules of use; OA articles are governed by the applicable Creative Commons License

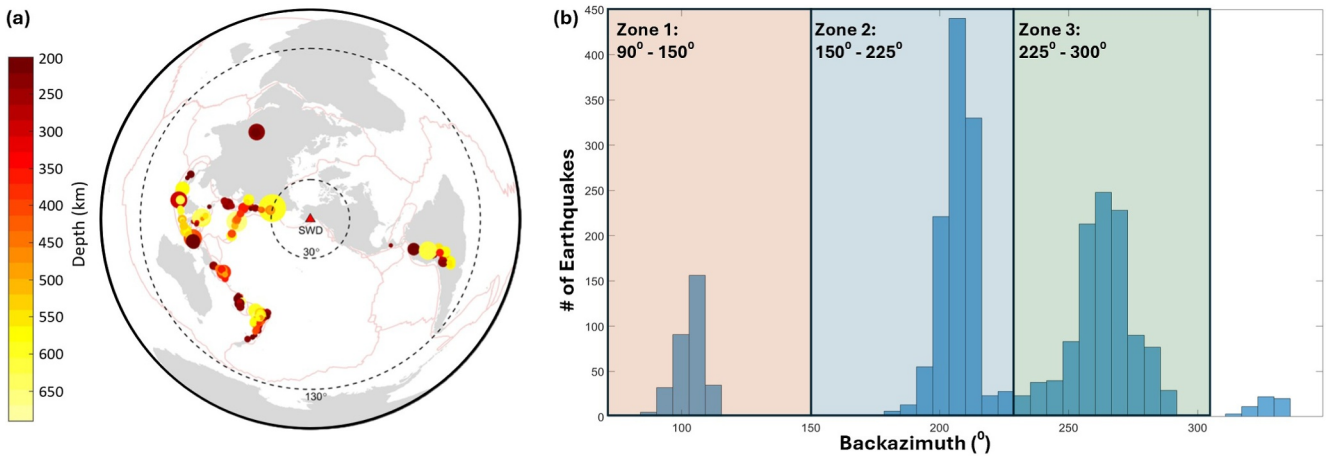

Figure 2. Global earthquake distribution used in this study. Panel (a) shows the earthquake locations using an equidistant azimuthal map. Colored dots indicate the focal depths, and the red triangle indicates station SWD in southern Alaska. Panel (b) shows a histogram of earthquakes by backazimuth. The three shaded regions highlight backazimuth Zones 1, 2, 3 as defined here and used for our analysis.

3. Results

3.1. Splitting Observations

Most of our high-quality SWS measurements correspond to SKS and SKKS phases (~1,820), while the remaining measurements are associated with S and ScS phases. To ensure comprehensive azimuthal coverage and to evaluate the backazimuthal dependency of SWS patterns, we included events spanning a backazimuth range 90°–300°, encompassing earthquakes from South America, Tonga, Java, and Japan.

This study focuses on the observation of the splitting parameters as a function of event backazimuth. We naturally categorize the earthquakes into three primary backazimuthal zones that we call Zone 1, Zone 2, and Zone 3, respectively: 90°–150°, 150°–225°, and 225°–300° (Figure 2). These teleseismic events are selected because their ray paths intersect the subducting slab before reaching the stations. The observed SWS patterns of earthquakes in the same backazimuthal zone show a high degree of spatial consistency (Figure S2 in Supporting Information S1). It motivated us to do averaging of the measurements. At each seismic station, we measured the splitting parameters for all events, then computed arithmetic and circular mean values of delay time and fast S polarization directions respectively, within the defined backazimuthal zones. The resulting averaged measurements for each station in backazimuthal sectors are illustrated in Figures 3a–3c. We can notice that the SWS patterns differ between backazimuthal zones (Figure 3) and demonstrate that these observed splitting patterns depend on the

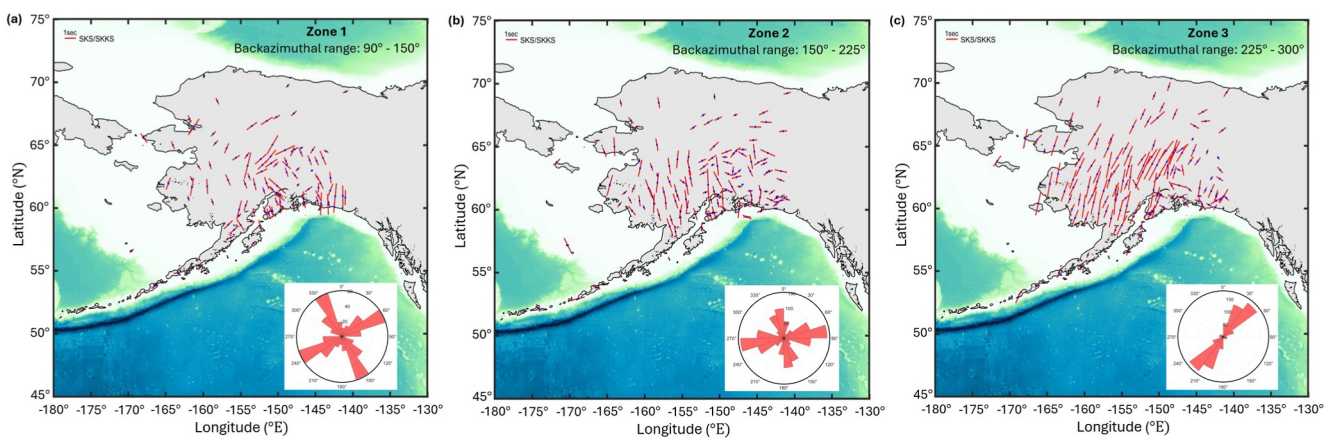

Figure 3. (a–c) Averaged SKS and SKKS shear wave splitting results of the three earthquake backazimuthal zones defined in Figure 2. The inset rose diagrams display the fast-S wave polarization directions of all stations, with the radius representing the number of measurements within each angular sector.

19448007, 2025, 20, Downloaded from https://agupubs.onlinelibrary.wiley.com/doi/10.1029/2025GL116411 by Yingcai Zheng - University of Houston , Wiley Online Library on [12/11/2025]. See the Terms and Conditions (https://onlinelibrary.wiley.com/terms-and-conditions) on Wiley Online Library for rules of use; OA articles are governed by the applicable Creative Commons License

19448007, 2025, 20, Downloaded from https://agupubs.onlinelibrary.wiley.com/doi/10.1029/2025GL116411 by Yingcai Zheng - University of Houston , Wiley Online Library on [12/11/2025]. See the Terms and Conditions (https://onlinelibrary.wiley.com/terms-and-conditions) on Wiley Online Library for rules of use; OA articles are governed by the applicable Creative Commons License

earthquake backazimuth. In addition, we also have limited S and ScS phase records shown in Figure S3 in Supporting Information S1. These backazimuth-dependent observations allow us to predict splitting patterns using a dipping intra-slab anisotropic model with different ray backazimuths and ray incident angles.

Our results show that delay times range from 0.5 to 1.5 s (Figure 3), suggesting the presence of a strong anisotropic source. We also observed that the fast-S wave polarization directions vary spatially across Alaska, with a notable pattern of orientations wrapping around the eastern margin of the Pacific-Yakutat slab, consistent with other studies (e.g., McPherson et al., 2020; Yang et al., 2021). Across the Alaska region, Zone 1 shows a widely scattered distribution of fast-S wave directions, with alignments generally trending NE–SW and NW–SE (Figure 3a). Zone 2 exhibits a similarly broad spread, with orientations trending approximately N–S and E–W (Figure 3b). In contrast, Zone 3 displays the most coherent pattern, with fast-S wave directions predominantly trending NE–SW across the region (Figure 3c). At the eastern edge of the slab (southeast Alaska), the delay times are smaller compared to central Alaska, and the fast-S directions lack a dominant orientation in all three back-azimuthal zones. These spatial variations suggest a marked influence of slab geometry, as the observed changes in fast-S wave orientations tend to align with the local slab strike.

3.2. Forward Prediction of SWS Parameters Using Intra-Slab Anisotropic Model

We investigated whether the intra-slab tilted transverse isotropy (TTI) anisotropy model by Li et al. (2018) could generate the observed complex SWS patterns. Here, TTI means the TTI (e.g., laminated fabric) with a symmetry perpendicular to the slab. Following Appini, Li, et al. (2025), we utilized full-wavefield modeling approach based on the propagator matrix method (Haskell, 1953; Mallick and Frazer, 1991). We simulated shear wave propagation through a simplified three-layered medium, with the central layer representing a dipping, anisotropic slab (Figure S1 in Supporting Information S1). We computed three-component synthetic seismograms for a range of plane wave incidence angles. To ensure the accuracy of our modeling, we also benchmarked our code against a finite difference implementation (Fang et al., 2017). These synthetic waveforms were then used to predict the delay time and fast orientation using the same SWS measurement techniques applied to our observed data set (see Section 2).

We constructed a forward seismological model for the Alaska subduction zone that includes a dipping anisotropic slab layer following the detailed Alaska-Aleutians slab geometry from the Slab2.0 model (Hayes et al., 2018). In general, to describe a TTI medium, we need the following: the symmetry axis (two angles), three anisotropy parameters (here, we use the notations of Thomsen (1986)), and P and S propagation velocities along the symmetry axis. In addition, we also need to set the TTI layer thickness. In our model, the symmetry axis is set to be perpendicular to the Alaska slab surface prescribed by Slab2.0, the shear anisotropy $\gamma \sim 0.3$ is constrained and from Li et al. (2018), and the thickness of the anisotropy layer in the slab is a free parameter, varying between 20 and 60 km based on information presented by Hayes et al. (2018). We set the other two Thomsen anisotropy parameters (Thomsen, 1986) to be $\varepsilon = 0.1$ (P anisotropy) and $\delta = 0.1$ as we are not able to constrain them. The subducting slab beneath Alaska is geometrically complex, with slab strike angles ranging from 180° to 320°, and average slab dip angles varying between 20° and 60°. For each earthquake-station pair, we utilized the CrazySeismic package (Yu et al., 2017), a 1-D ray-tracing algorithm, to locate the SKS ray piercing point on the slab interface and determine the local incident/transmission angle of the seismic wave. At each piercing point, we extracted the slab's local strike and dip to improve the accuracy of our SWS predictions. These structural parameters were further corroborated by comparison to the mid-slab surface model of the Alaska slab from Fuston and Wu (2020), which extends the slab model to deeper (~600 km) depths.

Combining this information, we computed synthetic waveforms for SKS propagation through the slab and applied the same rotation-correlation method to measure the predicted splitting parameters (fast-S polarization direction φ and delay time δt). Observed SWS patterns are highly consistent for multiple earthquakes within the same backazimuthal zone (Figure S2 in Supporting Information S1). Therefore, we selected one representative event from each zone to compare our model predictions against observations. Figure 4 shows the comparison of predicted versus observed SWS patterns in each backazimuthal zone. The agreement is excellent; for nearly all stations, the dipping anisotropic-slab model successfully reproduces the splitting patterns seen in the real data. Our synthetic results reproduce several key features observed in the data set, particularly the spatial variability in fast directions around the eastern slab edge. This supports the hypothesis that localized anisotropy within the slab contributes significantly to the observed splitting, particularly in complex areas such as the Pacific-Yakutat slab

10.1029/2025GL116411

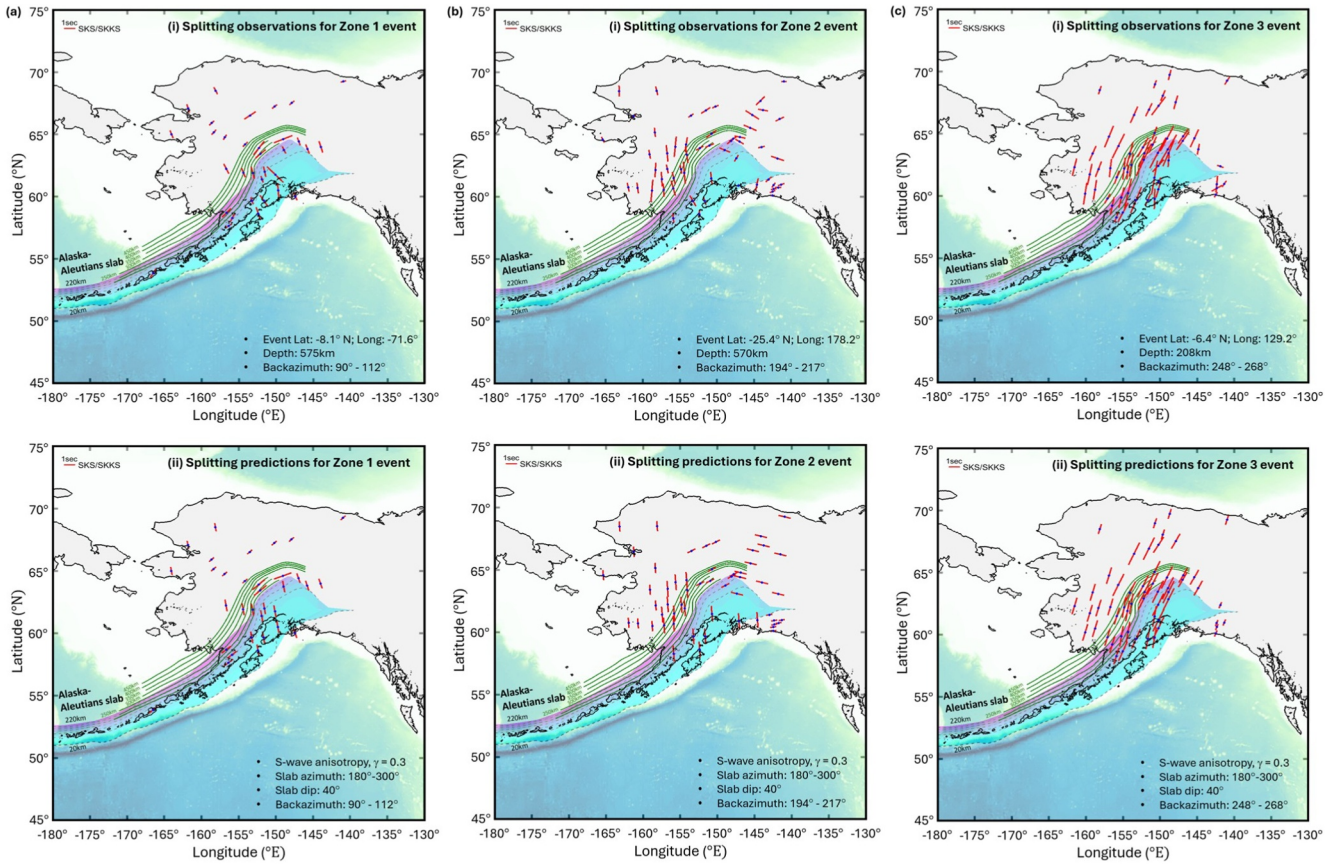

Figure 4. Observed versus modeled shear-wave splitting (SWS) patterns for representative earthquakes in backazimuthal Zones 1, 2, and 3 (see Figure 2). Panels (a–c) (i) display SWS measurements for a single earthquake in each zone, with event details noted in the lower right corner. Panels (a–c) (ii) show the corresponding synthetic SWS results generated using the same event information. The anisotropic model parameters: $\varepsilon = 0.1$ (P-wave anisotropy), $\gamma = 0.3$ (S-wave anisotropy) and the Thomsen's $\delta = 0.1$; and the elastic tensor used in this calculation are consistent with that of Appini, Li, et al. (2025). Green contour lines show top slab contours from Gou et al. (2019).

edge. Our model can also predict the observed delay times (up to 1.5 s), with residual delay times in the range 0.1–0.3 s. It may be due to crustal (C. Liu et al., 2024) and mantle wedge anisotropy (Hacker and Abers, 2012; Perttu et al., 2014) which are not considered here.

4. Discussion

The complexity of splitting patterns in Alaska has led previous SKS splitting studies to propose different mantle flow models and multi-layered anisotropy models (e.g., Christensen and Abers, 2010; Venereau et al., 2019; Yang et al., 2021). Some studies also speculated on the presence of fossil anisotropy within the subducting slab to explain the splitting trends closer to the trench (Christensen and Abers, 2010; Venereau et al., 2019). These studies converge on the idea that the Pacific-Yakutat slab significantly modulates mantle flow through its geometry, dip transition, and edge effects.

Complementing these observations, a few modeling studies have explored the mechanisms behind the observed anisotropy (e.g., Christensen and Abers, 2010). Song and Kawakatsu (2013) considered dipping anisotropy models to explain splitting patterns in Alaska. While our work shares similarities in this regard, there are some important differences. First, Song and Kawakatsu (2013) assigned the anisotropy mainly to sub-slab asthenosphere. They ruled out significant intra-slab contribution due to the then-limited evidence for strong anisotropy inside the slab. Our model was built on the current knowledge we have (Li et al., 2018), while still acknowledging possible contributions from the wedge and sub-slab regions. The predicted SWS patterns are natural consequences of our anisotropy model. Second, they used a line of stations, whereas the stations we used cover the entire Alaska slab. Third, the tectonic implications are different too. The sub-slab asthenosphere anisotropy (Song

19448007, 2025, 20, Downloaded from https://agupubs.onlinelibrary.wiley.com/doi/10.1029/2025GL116411 by Yingcai Zheng - University of Houston , Wiley Online Library on [12/11/2025]. See the Terms and Conditions (https://onlinelibrary.wiley.com/terms-and-conditions) on Wiley Online Library for rules of use; OA articles are governed by the applicable Creative Commons License

19448007, 2025, 20, Downloaded from https://agupubs.onlinelibrary.wiley.com/doi/10.1029/2025GL116411 by Yingcai Zheng - University of Houston , Wiley Online Library on [12/11/2025]. See the Terms and Conditions (https://onlinelibrary.wiley.com/terms-and-conditions) on Wiley Online Library for rules of use; OA articles are governed by the applicable Creative Commons License

and Kawakatsu, 2013) favors lattice preferred orientation of minerals possibly related to mantle flows. In our study, the strength of the inverted global S intra-slab anisotropy is independent of slab age, rate of subduction, or angle of subduction. It favors chemical and mechanical processes common to all types of subduction zones. The strong intra-slab anisotropy can be produced by aligned liquid/melt pockets embedded in sheet silicates such as serpentine group minerals (e.g., Li et al., 2018; Shirey et al., 2021). Highly deformed serpentine can exhibit shear-wave anisotropy as high as 32%, much stronger than olivine, which is consistent with the observed anisotropy in the Alaska subduction zone (Katayama et al., 2009). Furthermore, existence of aqueous water (or melt) in rocks can enhance seismic anisotropy via pore structure effect (Thomsen, 1995). Shear-wave anisotropy depends on pore aspect ratio, e, and volume fraction, f. It can be shown that aligned pore fluids in volume fraction $f \sim 1\%$ is sufficient to produce shear anisotropy 50%. In addition, mineral dehydration can enhance pore pressure and reduce effective pressure, which can enhance anisotropy as seen in the lab experiment by Carrasquilla et al. (2024).

There are also other works consistent with our intra-slab anisotropy model. Recent local splitting studies from intra-slab earthquakes (Karlowska et al., 2021; Richards et al., 2021) reveal fast directions that follow slab geometry. Karlowska et al. (2021) suggests that both forearc and backarc splitting mainly reflect slab anisotropy and a thin serpentinite layer atop the slab, with minimal mantle wedge influence. They also report smaller delay times (~0.3 s), likely because these local events sample only the upper part of the slab. Moreover, despite the shorter raypath, significant splitting has been observed even in the narrow layer between the earthquake source and slab top (Song and Kim, 2012), implying the presence of high anisotropy in thin intervals. This reinforces the plausibility of our TTI-based model, especially given the alignment between the fast-S polarization axes from both local and teleseismic measurements.

Our simplified intra-slab model can generate both the observed fast-S directions and delay times of the complex SWS patterns. There is a linear trade-off between anisotropy layer thickness and anisotropy strength, making it difficult to constrain them independently given the current ray coverage in our data set. Therefore, we fixed the shear anisotropy to be 0.3. Hence, it does not entirely rule out the possibility of additional anisotropic layers, such as the mantle wedge or the overriding lithosphere. However, our results indicate that the first-order SWS patterns in this region can be explained by the intra-slab TTI anisotropy alone. Additionally, our previous study (Appini, Li, et al., 2025) demonstrated through waveform modeling that source-side anisotropy has minimal influence on the observed SWS patterns. C. Liu and Ritzwoller (2024) inverted for regional 1-D layered models showing existence of TTI structure at shallower depth <50 km using surface waves. Integrating their models and our models could be a promising future research direction to understand anisotropy and associated Alaska mantle dynamics.

5. Conclusions

New modeling results combined with prior findings (Appini, Li, et al., 2025), show that strong intra-slab anisotropy subducting can account for observed SWS patterns which were previously attributed largely to mantle flow. This insight calls for a shift in how we interpret subduction zone SWS anisotropy and mantle flow dynamics. Rather than minimizing the role of slab anisotropy, we should consider its anisotropic structure (modeled here as TTI medium) as a key piece of the puzzle, despite the short ray path within the slab. Such a perspective can significantly alter existing geodynamic interpretations. For example, some trench-parallel splitting signals, historically thought to indicate trench-parallel mantle flow beneath the slab, are likely due to the orientation of anisotropic fabrics within the dipping slab. In Alaska, for all events with backazimuths between 90° and 300°, we observe systematic rotation of fast orientations aligned with the slab strike, with delay times ranging from 0.5 to 1.5 s. The strong dependence of these splitting patterns on backazimuth, along with the clear match between observed data and modeled predictions, provides a simple and compelling explanation for the observed splitting patterns. Although our focus is on slab anisotropy as an end-member model, the mantle wedge or sub-slab asthenospheric contribution may also play a secondary role. Our results will eventually enhance our understanding of slab structure and fabrics, mantle flow, and the mechanisms behind deep earthquake generation.

Conflict of Interest

The authors declare no conflicts of interest relevant to this study.

Data Availability Statement

The 3-component seismogram data utilized in this study is openly accessible through Incorporated Research Institutions for Seismology Data Management Center (IRIS-DMC, 2023). Data from the TA (Transportable Array, 2003) seismic network is made openly available as part of the EarthScope USArray facility, operated by IRIS (now EarthScope Consortium) and supported by the NSF EAR-1261681. IRIS Data Services are funded through the Seismological Facilities for the Advancement of Geoscience (SAGE) Award of the National Science Foundation under Cooperative Support Agreement EAR-1851048. The SplitLab software package, based on MATLAB, is available from Wüstefeld et al. (2008a, 2008b). We also provide our SWS processed results (including those shown in Figure S2 in Supporting Information S1) as a data set in the Excel file, deposited in the Texas Data Repository (Appini, Zheng, et al., 2025).

Acknowledgments

We are grateful to Dr. Carl Tape and the two anonymous reviewers for their insightful comments that helped refine our manuscript. We also appreciate the editor, Dr. Daoyuan Sun, for his guidance during the review process. This work is funded by NSF EAR-2027150 and USGS G22AC00428. WDM is supported by the US Geological Survey Earthquake Hazards Program USGS-2024-012. JW is supported by NSF EAR-1848327 and EAR-2422671.

References

Appini, S., Li, J., Hu, H., Creasy, N., Thomsen, L., McNease, J., & Zheng, Y. (2025). Prediction of complex observed shear wave splitting patterns at Ryukyu Subduction Zone using a strong intra-slab anisotropy model. *Geophysical Research Letters*, *52*(3), e2024GL111131. https://doi.org/10.1029/2024gl111131

Appini, S., Zheng, Y., Wu, J., & Mooney, W. D. (2025). Dataset: Teleseismic shear wave splitting measurements in Alaska (version 1.0) [Dataset]. *Texas Data Repository*. https://doi.org/10.18738/T8/ES5F5O

Beyreuther, M., Barsch, R., Krischer, L., Megies, T., Behr, Y., & Wassermann, J. (2010). ObsPy: A python toolbox for seismology. *Seismological Research Letters*, *81*(3), 530–533. https://doi.org/10.1785/gssrl.81.3.530

Bowman, J. R., & Ando, M. (1987). Shear-wave splitting in the upper-mantle wedge above the Tonga subduction zone. *Geophysical Journal International*, *88*(1), 25–41. https://doi.org/10.1111/j.1365-246x.1987.tb01367.x

Carrasquilla, M. D. L., Sun, M., Long, T., Sisson, V., Lapen, T., Jones, C., et al. (2024). Seismic anisotropy of granitic rocks from a fracture stimulation well at Utah FORGE using ultrasonic measurements. *Geothermics*, *123*, 103129. https://doi.org/10.1016/j.geothermics.2024.103129

Christensen, D. H., & Abers, G. A. (2010). Seismic anisotropy under central Alaska from SKS splitting observations. *Journal of Geophysical Research*, *115*(B4), B04315. https://doi.org/10.1029/2009jb006712

Dziewonski, A. M., Chou, T. A., & Woodhouse, J. H. (1981). Determination of earthquake source parameters from waveform data for studies of global and regional seismicity. *Journal of Geophysical Research*, *86*(Nb4), 2825–2852. https://doi.org/10.1029/jb086ib04p02825

Eakin, C. M., Long, M. D., Scire, A., Beck, S. L., Wagner, L. S., Zandt, G., & Tavera, H. (2016). Internal deformation of the subducted Nazca slab inferred from seismic anisotropy. *Nature Geoscience*, *9*(1), 56–59. https://doi.org/10.1038/ngeo2592

Eberhart-Phillips, D., Christensen, D. H., Brocher, T. M., Hansen, R., Ruppert, N. A., Haeussler, P. J., & Abers, G. A. (2006). Imaging the transition from Aleutian subduction to Yakutat collision in central Alaska, with local earthquakes and active source data. *Journal of Geophysical Research*, *111*(B11), B11303. https://doi.org/10.1029/2005jb004240

Ekström, G., Nettles, M., & Dziewonski, A. M. (2012). The global CMT project 2004–2010: Centroid-moment tensors for 13,017 earthquakes. *Physics of the Earth and Planetary Interiors*, *200*, 1–9.

Faccenda, M., Burlini, L., Gerya, T. V., & Mainprice, D. (2008). Fault-induced seismic anisotropy by hydration in subducting oceanic plates. *Nature*, *455*(7216), 1097–1098. https://doi.org/10.1038/nature07376

Fang, X. D., Zheng, Y. C., & Fehler, M. C. (2017). Fracture clustering effect on amplitude variation with offset and azimuth analyses. *Geophysics*, *82*(1), N13–N25. https://doi.org/10.1190/geo2016-0045.1

Frohlich, C. (2006). *Deep earthquakes*. Cambridge University Press.

Fukao, Y. (1984). Evidence from core-reflected shear-waves for anisotropy in the Earth's Mantle. *Nature*, *309*(5970), 695–698. https://doi.org/10.1038/309695a0

Fuston, S., & Wu, J. (2020). Raising the resurrection plate from an unfolded-slab plate tectonic reconstruction of northwestern North America since early Cenozoic time. *GSA Bulletin*, *133*(5–6), 1128–1140. https://doi.org/10.1130/b35677.1

Gou, T., Zhao, D., Huang, Z., & Wang, L. (2019). Aseismic deep slab and mantle flow beneath Alaska: Insight from anisotropic tomography. *Journal of Geophysical Research: Solid Earth*, *124*(2), 1700–1724. https://doi.org/10.1029/2018jb016639

Hacker, B. R., & Abers, G. A. (2012). Subduction factory 5: Unusually low Poisson's ratios in subduction zones from elastic anisotropy of peridotite. *Journal of Geophysical Research*, *117*(B6), B06308. https://doi.org/10.1029/2012jb009187

Haskell, N. A. (1953). The dispersion of surface waves on multilayered media. *Bulletin of the Seismological Society of America*, *43*(1), 17–34. https://doi.org/10.1785/bssa0430010017

Hayes, G. P., Moore, G. L., Portner, D. E., Hearne, M., Flamme, H., Furtney, M., & Smoczyk, G. M. (2018). Slab2, a comprehensive subduction zone geometry model. *Science*, *362*(6410), 58–61. https://doi.org/10.1126/science.aat4723

Haynie, K. L., & Jadamec, M. A. (2024). Implications of variable plate coupling versus Plateau buoyancy on subduction dynamics: A case study of the Yakutat Plateau in Alaska. In *Tectonics and seismicity of Alaska and Western Canada—EarthScope and beyond, geophysical monograph series* (pp. 355–387).

Incorporated Research Institutions for Seismology Data Management Center. (2023). IRIS-DMC [Dataset]. Retrieved from https://ds.iris.edu/ds/nodes/dmc/

IRIS Transportable Array. (2003). USArray transportable array [Dataset]. *International Federation of Digital Seismograph Networks*. https://doi.org/10.7914/SN/TA

Jin, Z., Yang, Y., Siregar, M. I., Mu, Z., Islam, S. M. A., Zhao, Q., et al. (2024). Seismic anisotropy and upper mantle dynamics in Alaska: A review of shear wave splitting analyses. *Earthquake Research Advances*, *4*(2), 100289. https://doi.org/10.1016/j.eqrea.2024.100289

Karlowska, E., Bastow, I. D., Rondenay, S., Martin-Short, R., & Allen, R. M. (2021). The development of seismic anisotropy below south-central Alaska: Evidence from local earthquake shear wave splitting. *Geophysical Journal International*, *225*(1), 548–554. https://doi.org/10.1093/gji/ggaa603

Katayama, I., Hirauchi, H., Michibayashi, K., & Ando, J. (2009). Trench-parallel anisotropy produced by serpentine deformation in the hydrated mantle wedge. *Nature*, *461*(7267), 1114–1209. https://doi.org/10.1038/nature08513

19448007, 2025, 20, Downloaded from https://agupubs.onlinelibrary.wiley.com/doi/10.1029/2025GL116411 by Yingcai Zheng - University of Houston , Wiley Online Library on [12/11/2025]. See the Terms and Conditions (https://onlinelibrary.wiley.com/terms-and-conditions) on Wiley Online Library for rules of use; OA articles are governed by the applicable Creative Commons License

Kirby, S. H., Durham, W. B., & Stern, L. A. (1991). Mantle phase changes and deep-earthquake faulting in subducting lithosphere. *Science*, *252*(5003), 216–225. https://doi.org/10.1126/science.252.5003.216

Levin, V., Margheriti, L., Park, J., & Amato, A. (2002). Anisotropic seismic structure of the lithosphere beneath the Adriatic coast of Italy constrained with mode-converted body waves. *Geophysical Research Letters*, *29*(22), 2058. https://doi.org/10.1029/2002gl015438

Li, J., Zheng, Y., Thomsen, L., Lapen, T. J., & Fang, X. (2018). Deep earthquakes in subducting slabs hosted in highly anisotropic rock fabric. *Nature Geoscience*, *11*(9), 696–700. https://doi.org/10.1038/s41561-018-0188-3

Liang, X., Zhao, D., Hua, Y., & Xu, Y. G. (2023). Big mantle wedge and intraplate volcanism in Alaska: Insight from anisotropic tomography. *Journal of Geophysical Research: Solid Earth*, *129*(1), e2023JB027617. https://doi.org/10.1029/2023jb027617

Liu, C., & Ritzwoller, M. H. (2024). Seismic anisotropy and deep crustal deformation across Alaska. *Journal of Geophysical Research: Solid Earth*, *129*(5), e2023JB028525. https://doi.org/10.1029/2023jb028525

Liu, C., Sheehan, A. F., & Ritzwoller, M. H. (2024). Seismic azimuthal anisotropy beneath the Alaska subduction zone. *Geophysical Research Letters*, *51*(14), e2024GL109758. https://doi.org/10.1029/2024gl109758

Liu, Z., Liang, C., Cao, F., Fan, X., & Chen, C. (2025). Mechanisms for layered anisotropy and anomalous magmatism of Alaska subduction system revealed by ambient noise tomography and the wave gradiometry method. *Journal of Geophysical Research: Solid Earth*, *130*(1), e2024JB029105. https://doi.org/10.1029/2024jb029105

Long, M. D., & Silver, P. G. (2009). Shear wave splitting and Mantle Anisotropy: Measurements, interpretations, and new directions. *Surveys in Geophysics*, *30*(4–5), 407–461. https://doi.org/10.1007/s10712-009-9075-1

Lynner, C., Long, M. D., Thissen, C. J., Paczkowski, K., & Montesi, L. G. J. (2017). Evaluating geodynamic models for sub-slab anisotropy: Effects of olivine fabric type. *Geosphere*, *13*(2), 247–259. https://doi.org/10.1130/ges01395.1

Lynner, C., Toro-Acosta, C., Paulson, E., & Birkey, A. (2024). Local-S shear wave splitting along the length of the Alaska–Aleutian subduction zone. *Geophysical Journal International*, *237*(3), 1567–1574. https://doi.org/10.1093/gji/ggae107

Mallick, S., & Frazer, L. N. (1991). Reflection-transmission coefficients and azimuthal anisotropy in marine seismic studies. *Geophysical Journal International*, *105*(1), 241–252. https://doi.org/10.1111/j.1365-246x.1991.tb03459.x

McPherson, A. M., Christensen, D. H., Abers, G. A., & Tape, C. (2020). Shear wave splitting and mantle flow beneath Alaska. *Journal of Geophysical Research: Solid Earth*, *125*(4), e2019JB018329. https://doi.org/10.1029/2019jb018329

Nowacki, A., Kendall, J. M., Wookey, J., & Pemberton, A. (2015). Mid-mantle anisotropy in subduction zones and deep water transport. *Geochemistry, Geophysics, Geosystems*, *16*(3), 764–784. https://doi.org/10.1002/2014gc005667

Perttu, A., Christensen, D., Abers, G., & Song, X. (2014). Insights into mantle structure and flow beneath Alaska based on a decade of observations of shear wave splitting. *Journal of Geophysical Research: Solid Earth*, *119*(11), 8366–8377. https://doi.org/10.1002/2014jb011359

Richards, C., Tape, C., Abers, G. A., & Ross, Z. E. (2021). Anisotropy variations in the Alaska subduction Zone based on shear-wave splitting from intraslab earthquakes. *Geochemistry, Geophysics, Geosystems*, *22*(5), e2020GC009558. https://doi.org/10.1029/2020gc009558

Savage, M. K. (1999). Seismic anisotropy and mantle deformation: What have we learned from shear wave splitting? *Rev Geophys*, *37*(1), 65–106. https://doi.org/10.1029/98rg02075

Sawade, L., Beller, S., Lei, W., & Tromp, J. (2022). Global centroid moment tensor solutions in a heterogeneous earth: The CMT3D catalogue. *Geophysical Journal International*, *231*(3), 1727–1738. https://doi.org/10.1093/gji/ggac280

Shirey, S. B., Wagner, L. S., Walter, M. J., Pearson, D. G., & van Keken, P. E. (2021). Slab transport of fluids to deep focus earthquake Depths—Thermal modeling constraints and evidence from diamonds. *AGU Advances*, *2*(2), e2020AV000304. https://doi.org/10.1029/2020av000304

Silver, P. G., & Chan, W. W. (1991). Shear wave splitting and subcontinental mantle deformation. *Journal of Geophysical Research*, *96*(B10), 16429–16454. https://doi.org/10.1029/91jb00899

Song, T.-R. A., & Kawakatsu, H. (2012). Subduction of oceanic asthenosphere: Evidence from sub-slab seismic anisotropy. *Geophysical Research Letters*, *39*(17), L17301. https://doi.org/10.1029/2012gl052639

Song, T.-R. A., & Kawakatsu, H. (2013). Subduction of oceanic asthenosphere: A critical appraisal in central Alaska. *Earth and Planetary Science Letters*, *367*, 82–94. https://doi.org/10.1016/j.epsl.2013.02.010

Song, T. R. A., & Kim, Y. (2012). Anisotropic uppermost mantle in young subducted slab underplating Central Mexico. *Nature Geoscience*, *5*(1), 55–59. https://doi.org/10.1038/ngeo1342

Thomsen, L. (1986). Weak elastic anisotropy. *Geophysics*, *51*(10), 1954–1966. https://doi.org/10.1190/1.1442051

Thomsen, L. (1995). Elastic anisotropy due to aligned cracks in porous rock. *Geophysical Prospecting*, *43*(6), 805–829. https://doi.org/10.1111/j.1365-2478.1995.tb00282.x

Venereau, C. M. A., Martin-Short, R., Bastow, I. D., Allen, R. M., & Kounoudis, R. (2019). The role of variable slab dip in driving mantle flow at the Eastern edge of the Alaskan subduction Margin: Insights from shear-wave splitting. *Geochemistry, Geophysics, Geosystems*, *20*(5), 2433–2448. https://doi.org/10.1029/2018gc008170

Walsh, E., Arnold, R., & Savage, M. K. (2013). Silver and Chan revisited. *Journal of Geophysical Research: Solid Earth*, *118*(10), 5500–5515. https://doi.org/10.1002/jgrb.50386

Wüstefeld, A., Bokelmann, G., Zaroli, C., & Barruol, G. (2008a). SplitLab: A shear-wave splitting environment in Matlab. *Computers & Geosciences*, *34*(5), 515–528. https://doi.org/10.1016/j.cageo.2007.08.002

Wüstefeld, A., Bokelmann, G., Zaroli, C., & Barruol, G. (2008b). SplitLab: A shear-wave splitting environment in MATLAB [Software]. *Montpellier Geosciences*. Retrieved from http://splitting.gm.univ-montp2.fr

Yang, Y., Gao, S. S., Liu, K. H., Kong, F., & Fu, X. (2021). Mantle flow in the vicinity of the Eastern edge of the Pacific-Yakutat slab: Constraints from shear wave splitting analyses. *Journal of Geophysical Research: Solid Earth*, *126*(9), e2021JB022354. https://doi.org/10.1029/2021jb022354

Yu, C., Zheng, Y., & Shang, X. (2017). Crazyseismic: A MATLAB GUI-Based software package for passive seismic data preprocessing. *Seismological Research Letters*, *88*(2A), 410–415. https://doi.org/10.1785/0220160207

19448007, 2025, 20, Downloaded from https://agupubs.onlinelibrary.wiley.com/doi/10.1029/2025GL116411 by Yingcai Zheng - University of Houston , Wiley Online Library on [12/11/2025]. See the Terms and Conditions (https://onlinelibrary.wiley.com/terms-and-conditions) on Wiley Online Library for rules of use; OA articles are governed by the applicable Creative Commons License